Supplement of Atmos. Chem. Phys., 24, 9435–9457, 2024
https://doi.org/10.5194/acp-24-9435-2024-supplement

Atmospheric Chemistry and Physics
Open Access
EGU

Supplement of

Distinct structure, radiative effects, and precipitation characteristics of deep convection systems in the Tibetan Plateau compared to the tropical Indian Ocean

Yuxin Zhao et al.

Correspondence to: Jiming Li (lijiming@lzu.edu.cn)

Region	Sample number	Width of DCSs (km) / SD	Width of DCCs (km) / SD	Width of anvil (km) / SD
TO	285	612.4/564.6	54.0/62.6	558.4/542.3
TP (total)	111	201.4/192.4	21.3/15.5	180.1/186.3
TP (NW)	10	198.2/133.2	14.6/5.8	183.6/132.1
TP (NE)	18	136.2/148.0	21.6/18.0	114.6/134.3
TP (SW)	35	225.3/220.4	22.2/15.4	203.1/215.7
TP (SE)	48	209.1/195.2	22.0/16.0	187.1/188.7

Region	DCCs /DCSs[a] (%)	Thickness of DCCs (km) / SD	DCCs/DCSs penetrating tropopause (%)	Mean precipitation of DCCs (mm hr^{-1})
TO	14.5	14.4/1.3	31.6/45.3	3.4
TP (total)	18.3	9.7/1.3	14.4/26.1	0.9
TP (NW)	14.0	9.1/1.3	20.0/20.0	0.2
TP (NE)	22.5	9.9/1.3	22.2/27.8	1.1
TP (SW)	18.6	9.7/1.4	14.3/25.7	0.6
TP (SE)	17.6	9.6/1.3	10.4/27.1	1.0

Table S1: Same to Table 2, but daytime (~1:30 p.m.) DCSs during 2006-2011.

Region	Sample number	Width of DCSs (km) / SD	Width of DCCs (km) / SD	Width of anvil (km) / SD
TO	357	725.4/592.6	72.1/73.8	653.3/574.5
TP (total)	10	974.3/856.0	37.0/30.4	937.3/865.8
TP (NW)	0			
TP (NE)	0			
TP (SW)	3	775.1/719.8	45.5/8.3	729.7/723.3
TP (SE)	7	1059.6/947.7	33.3/36.3	1056.3/958.8

Region	DCCs /DCSs[a] (%)	Thickness of DCCs (km) / SD	DCCs/DCSs penetrating tropopause (%)	Mean precipitation of DCCs (mm hr^{-1})
TO	16.5	14.7/1.5	40.6/54.9	4.0
TP (total)	9.2	11.4/1.9	20.0/30.0	2.0
TP (NW)				
TP (NE)				
TP (SW)	19.0	13.4/1.1	33.3/66.7	3.3
TP (SE)	5.0	10.5/1.5	14.3/14.3	1.4

Table S2: Same to Table2, but nighttime (~1:30 a.m.) DCSs during 2006-2011.

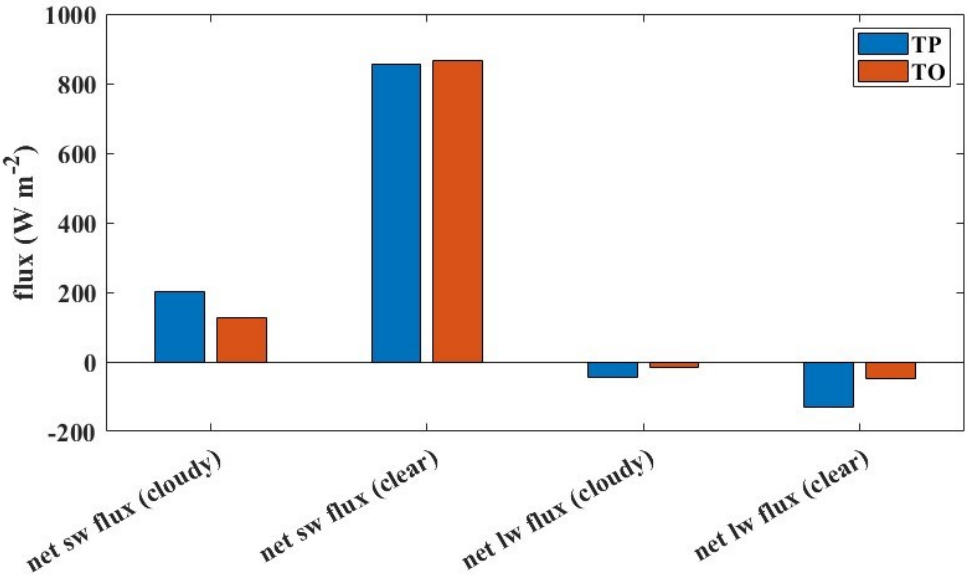

Fig. S1. The mean net SW flux (W m^{-2}) and LW flux (W m^{-2}) under cloudy (all-sky) or clear-sky conditions of DCCs in different regions at BOA.

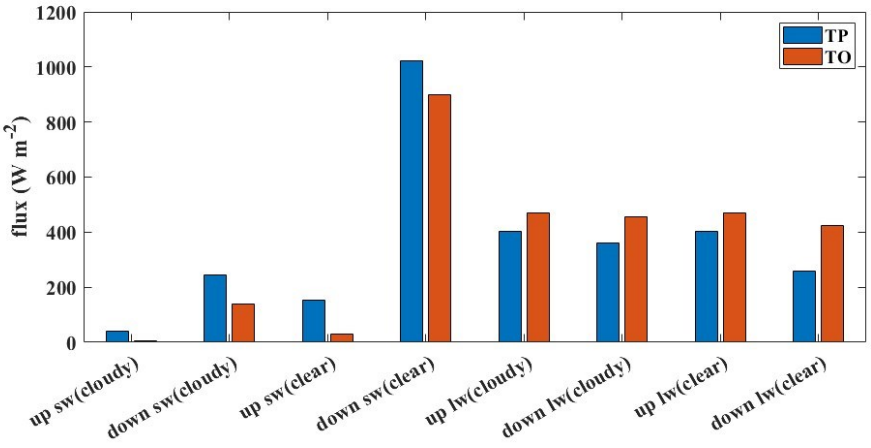

Fig. S2. The mean upwelling and downwelling SW flux (W m^{-2}) and LW flux (W m^{-2}) under cloudy (all-sky) or clear-sky conditions of DCCs in different regions at BOA.

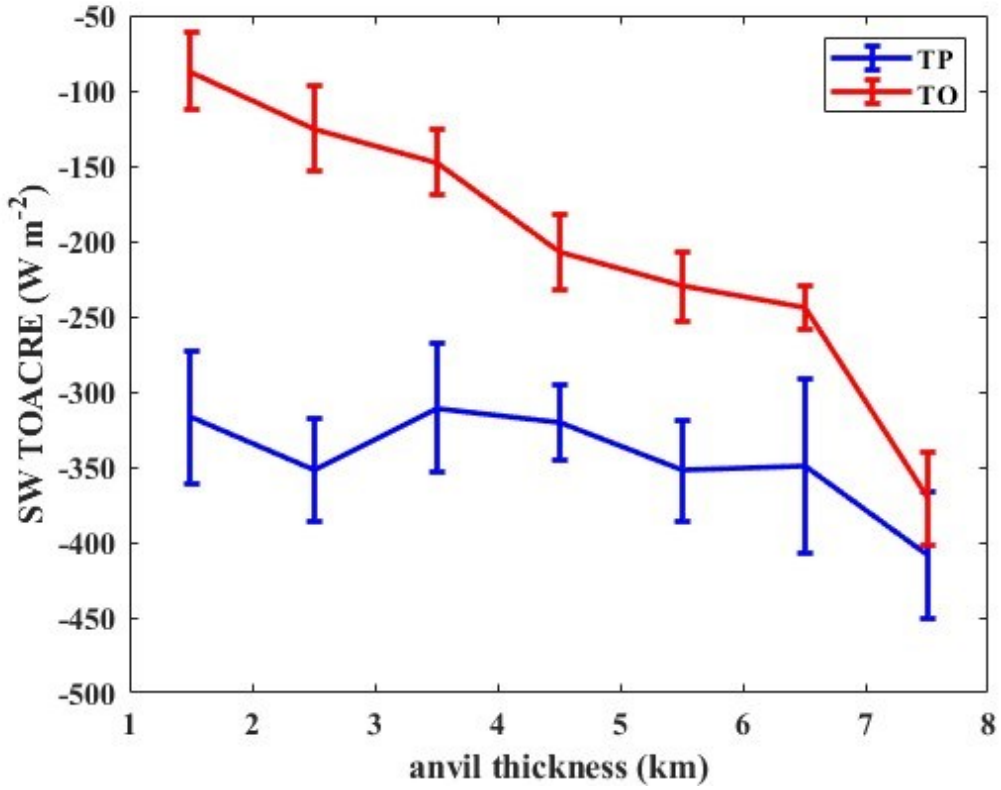

Fig. S3. Bin-averaged SW TOA CRE (W m^{-2}) of anvil and the thickness of anvil (km) in the TO. The error bars represent the standard error of the mean (SEM=standard error / √n).

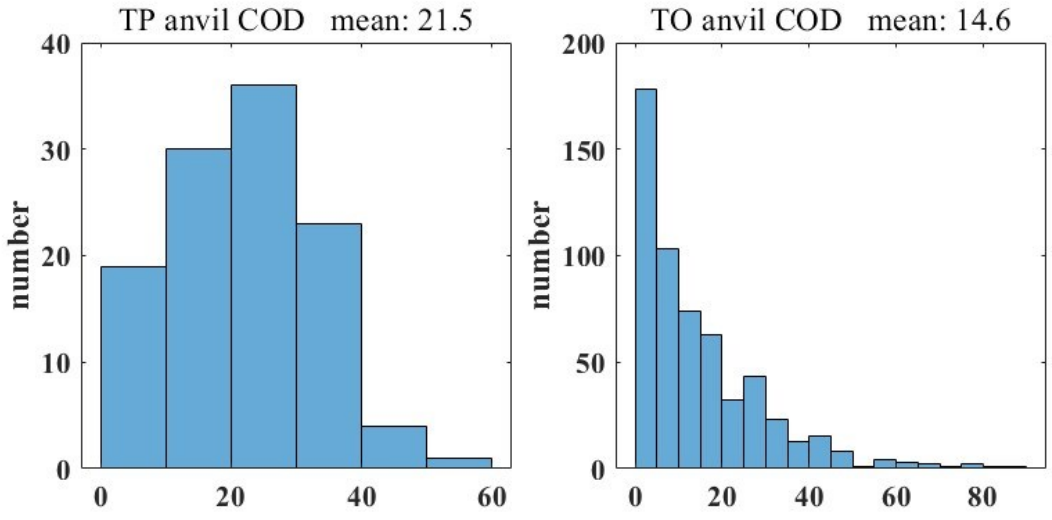

Fig. S4. The histograms and mean values of cloud optical depth of anvils in different regions. The data is from 2B-FLXHR-LIDAR datasets.

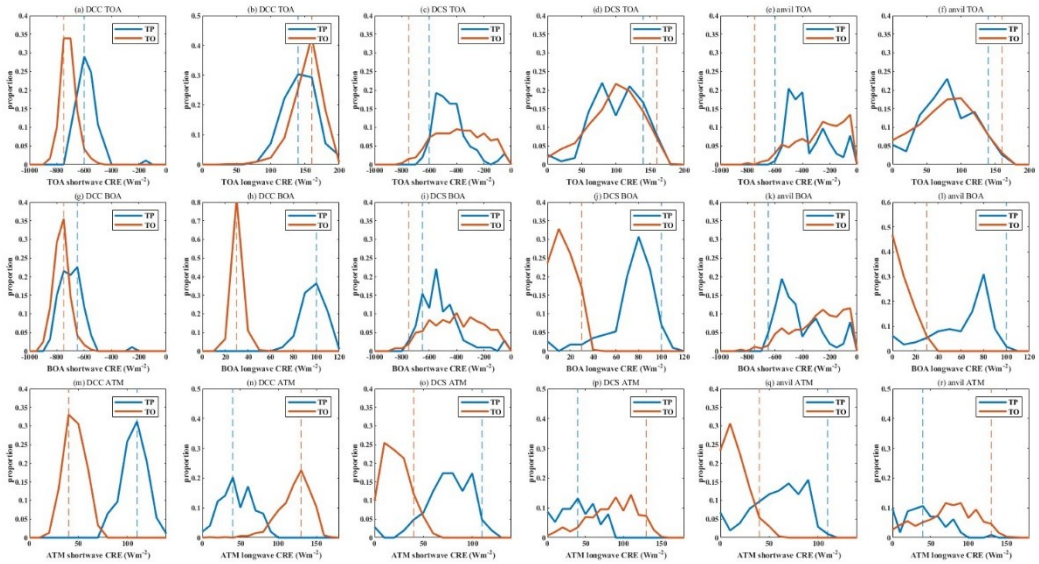

Fig. S5. The proportion of each bin of the LW CRE, the SW CRE at TOA, BOA, and ATM in the total sample of the TP (blue), and TO (red). The dash lines show the peak of DCC.

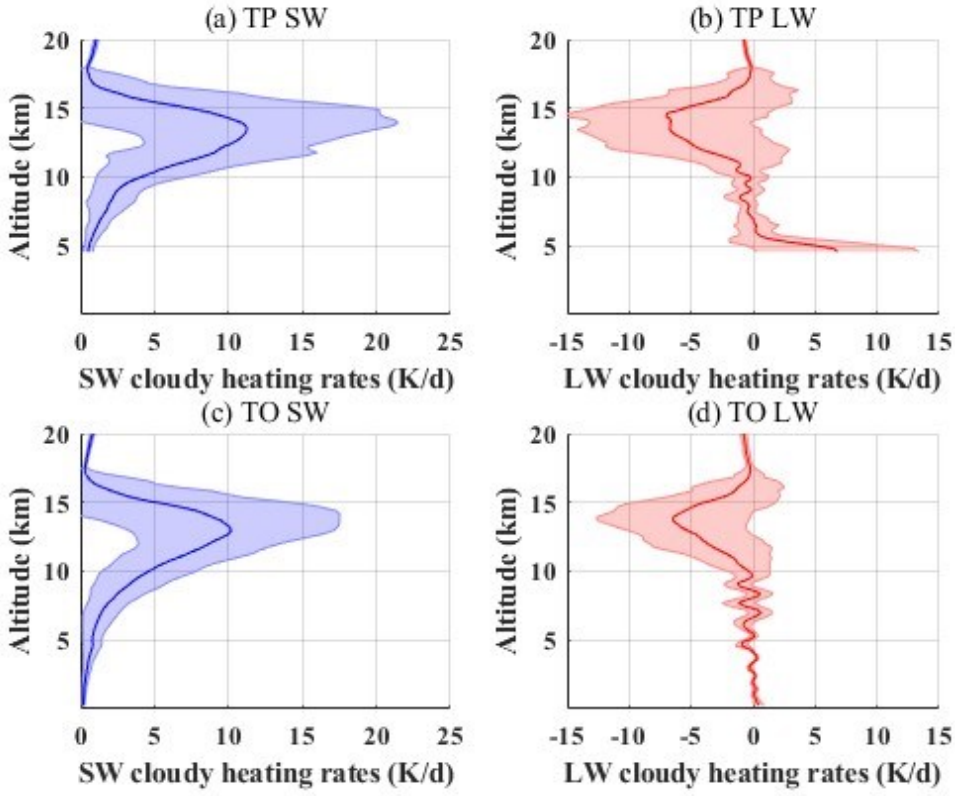

Fig. S6. The mean vertical profiles of cloudy (all-sky) heating rates (K d^{-1}) of DCCs over the TP, and TO. The shadow range represents the standard deviation.

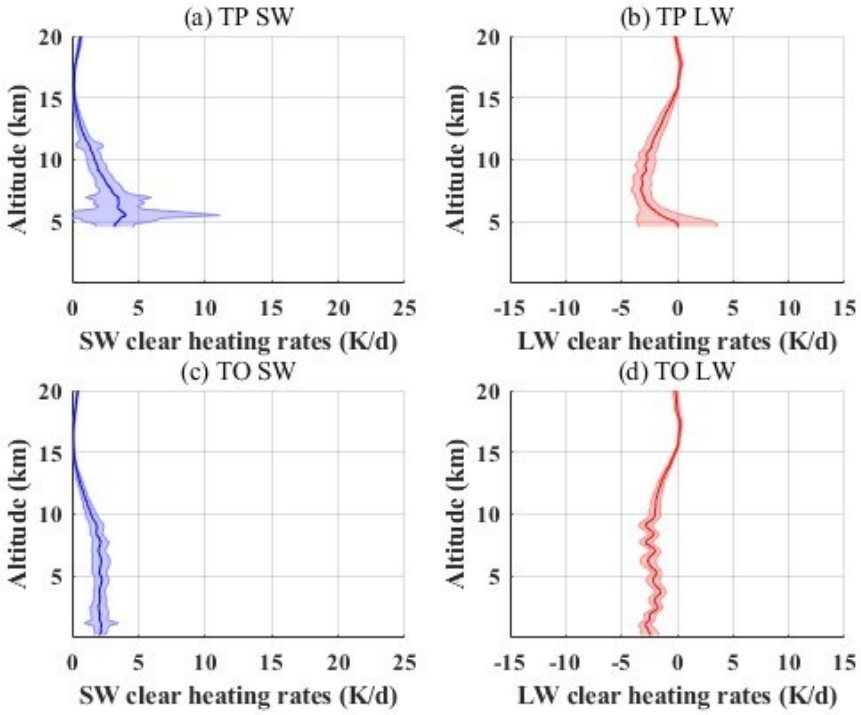

Fig. S7. The mean vertical profiles of clear-sky heating rates (K d^{-1}) of DCCs over the TP, and TO. The shadow range represents the standard deviation.

Region	TOA CRE (W m^{-2})					
	SWCRE			LWCRE		
	DCC	DCS	anvil	DCC	DCS	anvil
TP	-559.5	-418.0	-338.4	152.3	110.7	89.4
TO	-688.8	-348.8	-246.2	162.4	108.1	88.8
Region	BOA CRE (W m^{-2})					
	SWCRE			LWCRE		
	DCC	DCS	anvil	DCC	DCS	anvil
TP	-671.9	-498.0	-401.3	102.2	78.7	65.8
TO	-739.4	-375.4	-266.2	35.5	18.7	13.1

Table S3. The SW CRE (W m^{-2}) and LW CRE (W m^{-2}) at TOA and BOA of DCSs, DCCs and anvil in different regions.

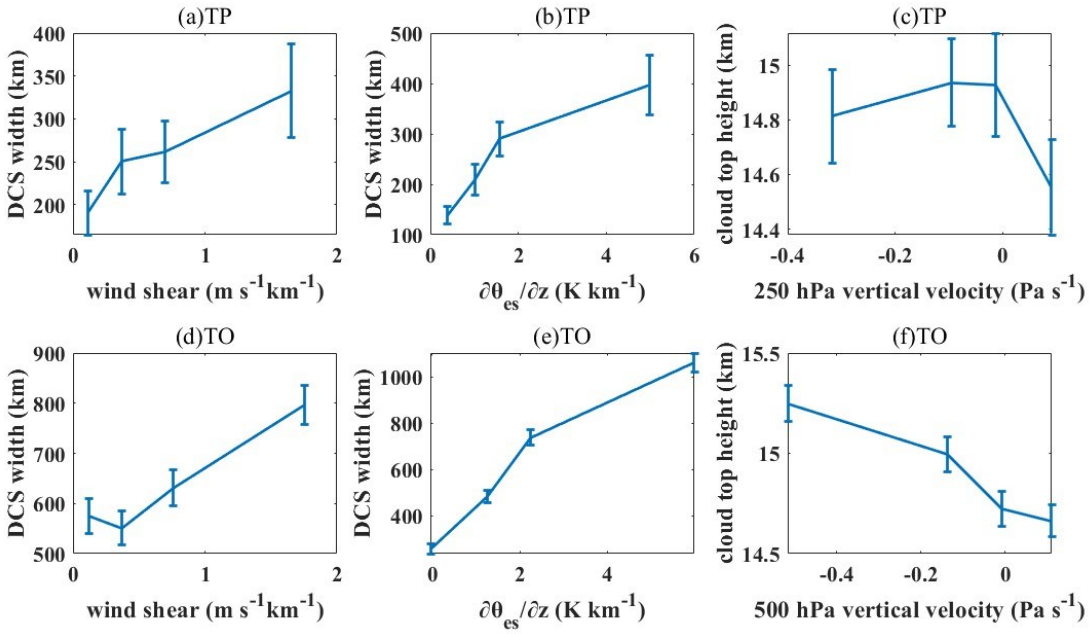

Fig. S8. Bin-averaged wind shear (m $s^{-1}km^{-1}$; a, d), the vertical gradient of the saturated equivalent potential temperature $\partial\theta_{es}/\partial z$ (K km^{-1}; b, e) and vertical velocity (Pa s^{-1}; c, f) with DCSs width (km) and cloud top height (km) from different regions. The error bars represent the standard error of the mean (SEM=standard error / $\sqrt{n}$).

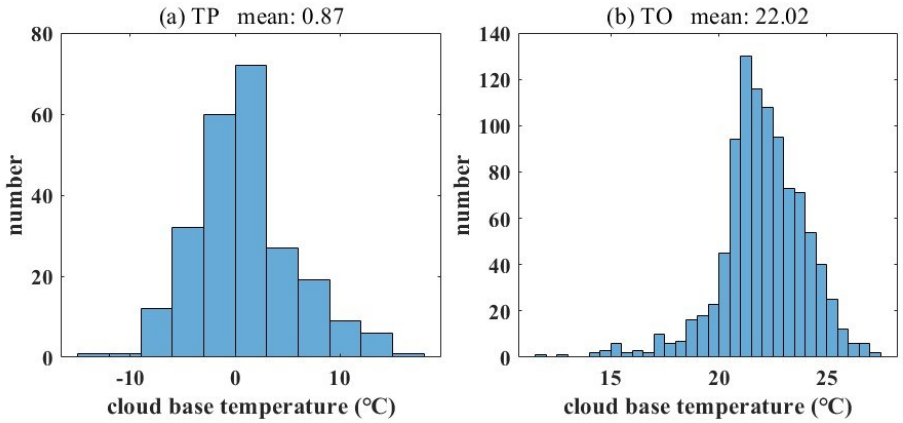

Fig. S9. Histogram of cloud base temperature (℃) of DCCs in the TP (a), and TO (b). And the mean cloud base temperature (℃) of DCCs in different regions.

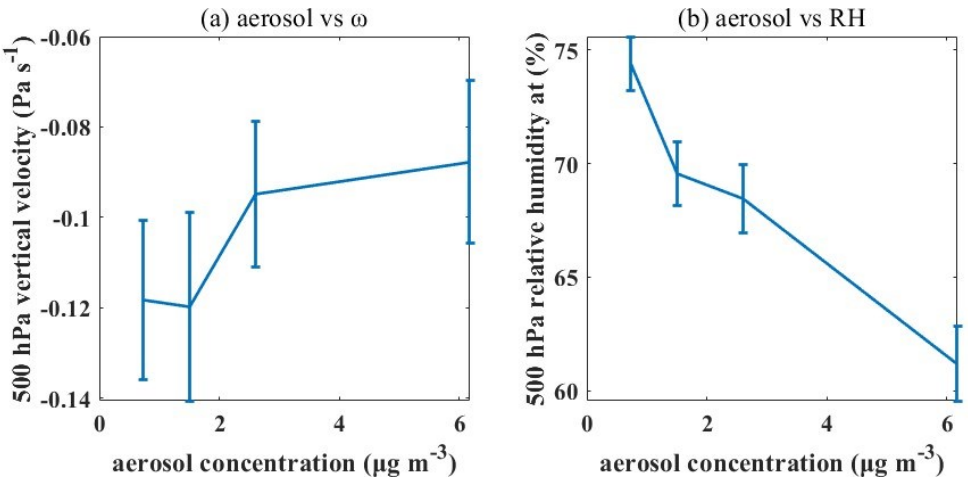

Fig. S10. Bin-averaged 500 hPa vertical velocity (Pa s^{-1}; a) and 500 hPa relative humidity (%; b) with aerosol concentration (μg m^{-3}) of DCCs in the TO. The error bars represent the standard error of the mean (SEM=standard error / $\sqrt{n}$).